

# CONTROLLED SLIDING LOCOMOTION FOR LEGGED ROVERS ON STEEP TERRAIN DURING SPACE EXPLORATION

Victor Barasuol<sup>1</sup>, Matteo Villa<sup>1</sup>, Marco Marchitto<sup>1</sup>, Gianluca Cerilli<sup>1</sup>, and Claudio Semini<sup>1</sup>

<sup>1</sup>*Istituto Italiano di Tecnologia (IIT), Dynamic Legged Systems lab, Via S. Quirico 19d, 16163 Genoa, Italy, claudio.semini@iit.it*

## ABSTRACT

Planetary exploration is a topic of great interest. A key challenge with today's wheeled rovers is limited mobility over rough terrain. Legged rovers can represent a valid solution compared to wheeled and flying robots, combining versatile mobility with payload capacity. In this paper, we present a novel concept of sliding locomotion on steep terrain. We designed a new type of robot torso that allows the legged robot to slide on it, as well as a new controller that allows steering, braking and thrusting commands by using the legs. We modified an Aliengo quadruped robot and tested it first in a lab environment on flat ground and then on a 10m tall pile of pebbles with an average inclination of 33°. To the best knowledge of the authors, this is the first time a controlled sliding locomotion has been presented and tested for legged robots.

Key words: Planetary Robotics; Legged Rover; Craters.

## 1. INTRODUCTION

One of the key challenges for planetary exploration with today's rovers is their limited mobility over rough terrain. Wheeled rovers have always been the preferred type of locomotion of all rovers deployed on the Moon and Mars so far, with the exception of Ingenuity, the Mars helicopter that has been operational since April 2021. While wheeled rovers have difficulties to access scientifically interesting areas like steep craters and caves, helicopters have limited battery run time and small payload. Legged Rovers are a promising addition to the wheeled robots and helicopters, since they combine rough terrain mobility with high payload capacity.

Moon craters, for example, are scientifically interesting because most of them were created more than two billion years ago. Some of them are in permanent darkness and thus a potential source of water ice. Moon's Shackleton crater for example has an average wall slope of 31°, that very rarely exceeds 35° [1]. The top and bottom of the walls show a smooth change in slope from a 35° wall to almost flat at the bottom of the crater.



Figure 1. Picture of the Aliengo quadruped robot with novel, custom-designed torso (design 2) lying on a pile of pebbles with retracted legs.

ESA and NASA, as well as other space agencies, have been financing several legged rover development projects over the past decades. In the recently concluded ESA-project *ANT*, the partners DFKI, IIT and Airbus collaborated to develop software and to test quadruped and hexapod rovers on steep crater analogues with a maximum inclination of 30° [2]. Researchers at ETH Zurich tested two types of quadruped robots on inclined terrain analogues with different soil types and a maximum slope of 25° [3]. Researchers at DFKI developed and tested several legged robots, like Scorpion [4], an octopod, and Mantis [5], a hexapod capable of choosing two types of postures: one optimized for locomotion (all the limbs are used to navigate) and another one for manipulation (the four back limbs are used for locomotion, and the two front ones for manipulation). The hexapod robot SpaceClimber was also tested in 2013 on sandy and inclined terrain [6]. Another example of bioinspired robot is Lauron V [7], developed by Research Center for Information Technologies (FZI). This hexapod, inspired by the stick insect morphology, has the ability to shift its center of mass such that it can walk with the four hind limbs, while manipulating object with the front ones. Bert [8], developed by the German Aerospace Center (DLR), is an extremely light-weight robot (3kg) that uses elastic actu-

ation for the locomotion, and it is able to traverse lava sand terrain with slope up to  $27.5^\circ$  before starting to slip.

Nasa Jet Propulsion Laboratory (JPL) has realized alternatives to wheeled locomotion too. The Axel family of rovers [9] tries to overcome the limitations of the wheeled mobility in steep slopes. Such robots behave as ordinary wheeled rovers over non steep terrain. When approaching to a steep slope, the Axel rover can set an anchor and descend the slope by deploying the tether stored inside the Axle. However, they still have the same difficulties of wheeled rovers when navigating in a rough and uneven terrain. Nasa JPL has also developed in the past decades legged robots for planetary exploration. Lemur [10] is a four-legged robot with grippers having micro spines, suitable for climbing rock walls. ATHLETE [11] and RoboSimian [12] have, respectively, six and four limbs, with wheels as end-effectors, which have demonstrated great performance over slightly unstructured and rough terrains.

The robots with six or eight legs introduced before are more stable during walking compared to four-legged systems. However, they in general have higher total robot mass and greater control complexity due to the higher number of joints. Moreover, they also have a higher number of components that might fail.

This paper presents the concept of a novel type of locomotion on steep terrain, preliminary hardware and software developments, as well as field test results. We developed controlled sliding locomotion on a custom-designed robot torso that allows a legged robot to efficiently descend a steep crater wall (Figure 1). The legs are retracted and lifted off from the ground while the robot is lying on the torso. A new sliding control system allows the robot to steer, brake and thrust during descending motions. To the best knowledge of the authors, this is the first time a controlled sliding locomotion has been presented and tested for legged robots.

The remainder of this paper is organized as follows: Section 2 presents the three different versions of the mechanical designs of the developed torso. Section 3 explains the details of the sliding locomotion control, including steering, braking and thrusting. Section 4 describes the experimental results of the multi-days field test campaign. Section 5 ends the paper with conclusions and future works.

## 2. TORSO DESIGN

A custom-shaped lower torso for Unitree's quadruped robot Aliengo was designed. As shown in Figure 2, three different designs were investigated; the first two differ in their round front for a low-resistance descent whilst the third one adds skids for steering capabilities. The parts were printed using the filament Ultem™ 9085 in the Stratasys Fortus 400 printer and bolted to the main body of the robot. The selected material is a high-performance thermoplastic with high strength-to-weight

ratio and high impact resistance ideal for this sort of application. The torso allows the 4 legs to move without restricting their workspace during descending; maximizes the contact area with the ground to reduce the sinking of the robot when sliding and has low-radius lateral bends to increase steering capabilities and maintain trajectories non-colinear to the descending direction. Since the maximum printable volume of the 3d printer Fortus 400 is 406mm x 355mm x 406mm, the lower torso was split and printed in two halves which were then glued together using the epoxy Resin Loctite 9480. This allowed also to reuse the rear part of the lower torso when the second and third design iterations were tested. The lower torso has a constant wall thickness of 4mm and a weight of about 1.4kg.

The first design iteration shown in Figure 2-1 is the one with the simplest geometry, flat on the bottom, front wall with a draft of  $40^\circ$  and radius of 100mm and side walls with a draft angle of  $10^\circ$ . This part was clamped to the torso of the robot without any horizontal gap in between.

The second design iteration shown in Figure 2-2 aimed at lowering the sinking of the front side of the robot observed when using the lower torso shape described in the first design iteration. The length of the front area was extended, inclined upwards by  $30^\circ$ , tapered and given a radius of 200mm. Spacers with a height of 30mm were added in between this part and the torso, because of the inclination given to the front side.

In the third design iteration shown in Figure 2-3 triangular skids were added to the rear side of the lower torso, described in the second design iteration, to increase sinking and lateral reaction forces between the ground and the lower torso to maintain a transversal trajectory to the slope when descending.

## 3. SLIDING LOCOMOTION CONTROL

The sliding control system is composed of three main commands: steering, braking, and thrusting. All the commands are executed using the legs and the concept of impedance control, where each foot receives desired position and velocity references according to each sliding control command. Figure 3 illustrates how the legs are used, as well as the most important parameters that affect the sliding posture and each leg motion generation for steering, braking, and thrusting.

The four robot legs are labeled as Left-Front (LF), Right-Front (RF), Left-Hind (LH), and Right-Hind (RH). All parameters and position vectors shown in Figure 3 are described in terms of each corresponding leg hip position and all values are referenced in the robot's Base Coordinate Frame (BF).

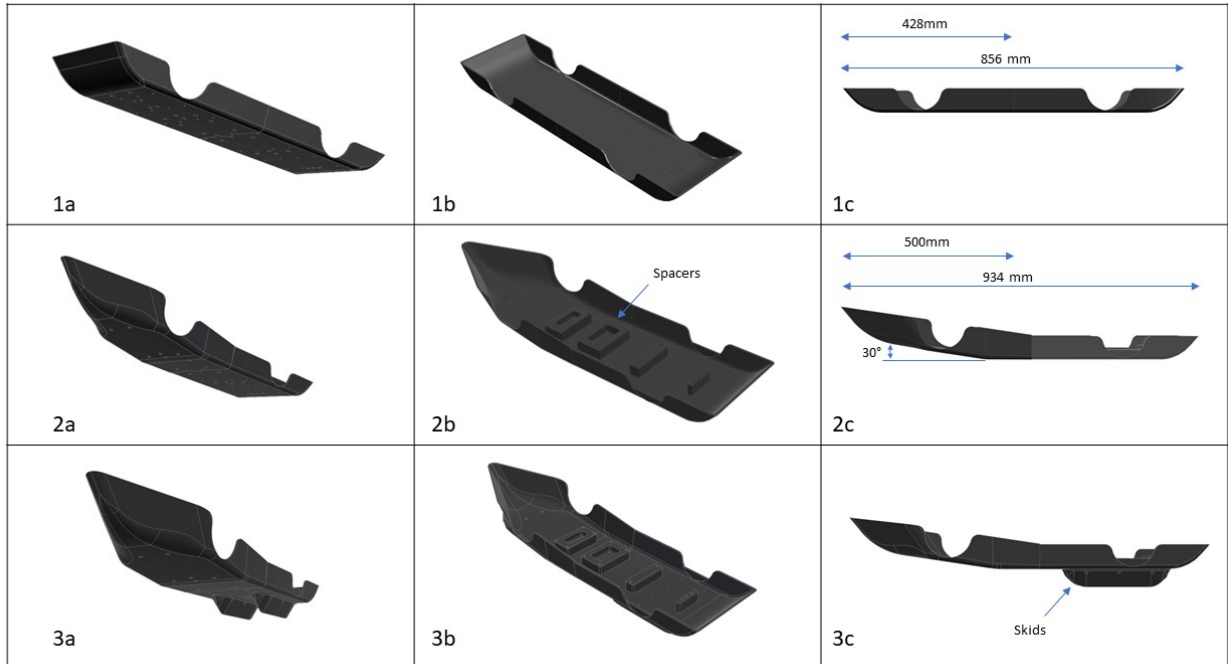


Figure 2. Three different designs of the lower torso. Row 1 shows the first design iteration with relatively simple and flat geometry, row 2 shows the second design iteration with tapered and inclined front and row 3 shows the third design iteration with skids mounted on the back.

### 3.1. Sliding posture

The robot's nominal posture during sliding (i.e., the robot's posture when no commands are being given) is defined by four position vectors:  $P_{LF}$ ,  $P_{RF}$ ,  $P_{LH}$  and  $P_{RH}$  (Figure 3). The procedure to choose the sliding posture takes two important aspects into consideration. The first aspect is the undesired interaction between the feet and the ground during pure sliding. The clearance between the feet and the ground must be enough to prevent contact interaction that can happen due to the partial sinkage of the torso. Such undesired contact interaction can slow down the robot's velocity and also create disturbances in the robot's heading. The second aspect regards the motion of each leg. The nominal posture determines the initial position of each foot and therefore the initial position of the foot trajectory of each of the three commands. As a consequence, it has a direct impact on the initial path of the foot trajectory. Thus, the sliding posture should also be defined to prevent each leg from reaching workspace limits or making the leg motion generation more complex around the initial path of the foot trajectory.

### 3.2. Steering, braking, and thrusting

For the steering, braking, and thrusting we implemented a simple motion generator that provides kinematic references at the Cartesian level. Inverse kinematics are

used to compute the corresponding joint references that are tracked with a joint-space impedance controller. For steering and braking, our motion generator produces a leg push motion. The direction of the leg push and the length of the leg stretching define whether the robot is steering or braking. The right-hind and left-hind legs move downwards and outwards to steer, respectively, to the right (Figure 3c) and to the left (Figure 3d). Both hind legs are commanded to move downwards to slow down the sliding motion (Figure 3e). The parameters that define the pushing motion for the steering and braking are  $d_x$ ,  $d_y$ , and  $d_z$ , which are quantities related to Cartesian coordinates expressed in the robot's base coordinate frame. The pushing reference trajectory of each foot is generated by means of a step input reference signal.

For thrusting, in case the sliding velocity must be sped up, the front legs perform a synchronized swimming motion (Figure 3b). The swimming motion is generated by means of a deformed circular motion in the sagittal plane, where the amplitude with respect to its origin varies according to the quadrant of the trajectory. The parameters that defined the shape of the circular trajectory are  $h_{down}$ ,  $h_{top}$ ,  $l_{front}$ , and  $l_{back}$ .

Since the contact interaction between the terrain surface and the robot feet are unknown and dynamic, the steering, braking and thrusting forces are managed through the joint impedance controller.

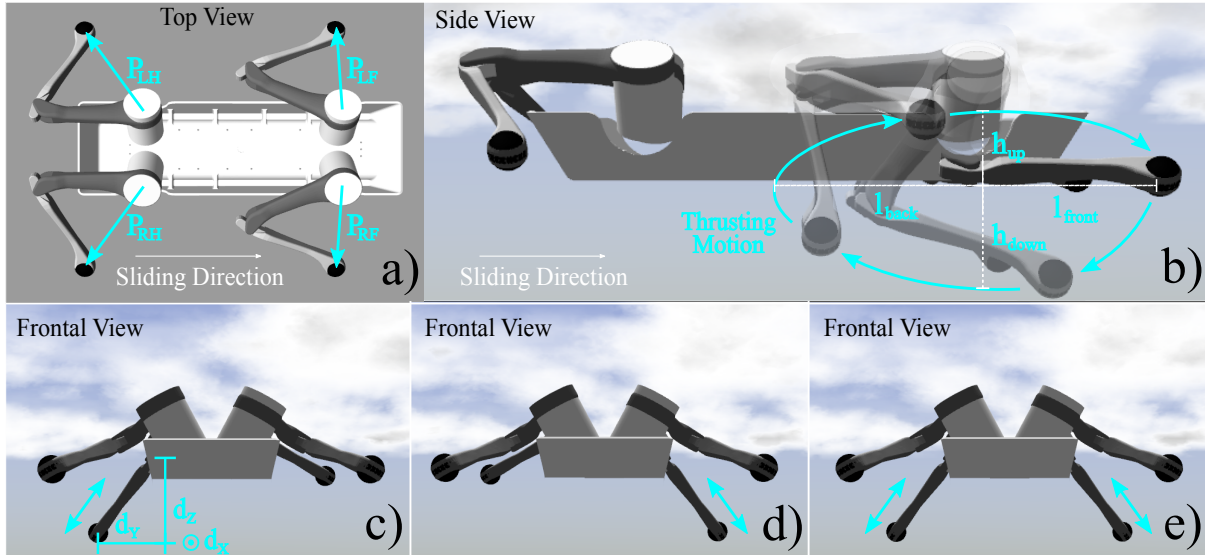


Figure 3. Illustration of the three sliding control commands as described in Section 3.

#### 4. EXPERIMENTAL RESULTS

This section describes the experimental results performed to assess the new torso designs (Section 2) and the implemented sliding locomotion controller (Section 3). The first section introduces details about the field test location and the robot platform, followed by the presentation of the results of two studies to assess the performance of the torso design and controller. Prior to the field tests, we tested the new leg motions in simulation, as well as in a lab environment with the robot lying on its torso on flat ground.

The videos of the experiments presented in this section can be found on our publications webpage at: <https://dls.iit.it/publications>.

##### 4.1. Field test location and robot platform

We performed a multi-days field test campaign in a suitable location close to IIT in Genoa that is part of a company producing construction aggregate, such as coarse-to medium-grained particulate material used in construction, including sand, gravel, etc. (Figure 4). In particular, we tested the robot on an approximately 10m tall pile of pebbles with a grain diameter between 8 and 15mm. During and between the days of the field trials, the company sporadically removed pebbles from the bottom of the pile and added new pebbles on the top, resulting in a fresh slope with an average critical angle of repose (i.e. the steepest angle of descent relative to the horizontal plane on which the material can be piled without sliding down) of  $33^\circ$ .

Even though the outdoor test location did not feature any instrumentation such as motion tracking and fixed cam-

eras, it allowed testing the robot on a steeper inclination than achievable in indoor Mars analogues with tilting platforms, such as the ones available at ALTEC in Torino (Italy) [13] or RUAG Space (Switzerland) [14], that have a maximum tilting angle of  $25^\circ$ .

Our experimental robot platform is the commercially available quadruped robot Aliengo from Unitree [15]. The robot has 3 active degrees of freedom in each leg and weighs 21kg. We modified the robot by mounting our custom-designed torso in the bottom of the robot, as well as an Intel NUC 11 computer on its back for additional computational power.



Figure 4. Picture of the field trial location close to IIT, in Genoa. The outdoor test campaign was performed on the  $33^\circ$  inclined pile of pebbles visible in the back.

## 4.2. Sliding performance of 3 different torso designs

In our first experimental trials, we tested the three different torso designs presented in Section 2. We are interested to understand the sliding performance of each design in terms of maintenance of steering capabilities and sliding friction.

From the experiments performed with the first and simple torso design, shown in Figure 5, we observed that the flat shape produced an increasing dragging force as it slides down the pile of pebbles. This increasing force is created by the accumulation of pebbles in the frontal part of the torso due to its flat shape, which ends up acting like a wall. Such accumulation of pebbles in the frontal part also increases the relative sinkage of the torso and undesired contact between the frontal feet and the ground. This accumulation of pebbles is clearly seen in the last image of the sequence (the last image on the right) depicted in Figure 5. Due to the substantial drag, the robot was only able to complete the descent by executing the leg swimming motion to thrust.

The second design showed much superior performance in terms of dragging when sliding down. The image sequence of this experiment is depicted in Figure 6. The frontal part was tapered and inclined to reduce dragging effects and prevent the accumulation of pebbles in the frontal part. The robot could complete the descent with a fast sliding speed and without the need of the leg motion to thrust. The high sliding velocity the robot achieved can be noticed by the time between each image of the sequence, which in this case is 0.75 seconds.

Regarding the sliding performance, the third design stays in between the first and second ones. The inclusion of skids has a visible impact on the maximum speed the robot can achieve. The image sequence extracted from the video of the experimental trial is depicted in Figure 7. In this case, the time between frames is 1.25 seconds. There was no need to perform any thrusting motion to reach the same approximate final descent position.

## 4.3. Assessing steering, braking and thrusting commands

The capabilities of the robot for steering, braking, and thrusting (Section 3) were assessed for the three lower torso designs. The sliding parameters (Figure 3) considered for the trials are shown in Table 1 (all values expressed in meter unit). The swimming frequency of the front legs for the thrusting was chosen to be 1.75 Hz. All the sliding locomotion control parameters reported in Table 1 are scaled between 0 to 100% of their values according to the user joystick commands used to operate the robot remotely.

The steering motion presented to be the most difficult to perform. It was very sensitive to the leg pushing parameters and to the shape of the lower torso. The best per-

	$d_x$	$d_y$	$d_z$	$h_{up}$	$h_{do}$	$l_{fr}$	$l_{ba}$
Steering	0.1	0.3	0.2	-	-	-	-
Braking	0.0	0.0	0.3	-	-	-	-
Swimming	-	-	-	0.02	0.25	0.05	0.35

Table 1. Sliding locomotion control parameters.

formance was achieved with the second design with tapered and inclined front. This design presented much less opposing forces to the steering motion, followed by the first and third design. Such opposing forces, that can be considered as torsional friction forces between the torso and the ground, were much more substantial for the third design due to the presence of the skids. With the third design the robot could barely twist, suggesting that the shape of the skids must be reviewed taking into account the trade-off between the torsional friction and the maintenance of the sliding direction on the incline.

The braking motion is the least problematic of the three commands in terms of performance. Even with the second design, which presented the lowest sliding friction, the robot was able to slow down and, if desired, stop the motion when the command was given. For the first design, the braking actions showed to be oversized due to the excessive dragging forces caused by the accumulation of pebbles in front of the torso. In this case, the corresponding leg pushing parameter  $d_z$  could be decreased to reduce the command sensitivity and the joint torques.

The thrusting performance assessment follows very similar observations as for the braking motion in terms of torso design. An important difference to highlight was the increase, from the second design, in the leg clearance from the ground. This modification increased the leg workspace free of ground interference and allowed for a more effective swimming motion.

We noticed during the experiments that partial surface collapse events represent a major challenge for controlling the sliding motion. This means that, if one of the three actions, or a combination of them, together with the dragging forces between torso and ground, create a partial ground collapse (local avalanche), the sliding controllability might be completely lost.

## 5. CONCLUSIONS

In this paper, we present a novel concept of sliding locomotion on steep terrain for legged rovers. To slide down a steep slope, a custom-designed lower torso was developed, for the quadruped robot Aliengo, to have efficient sliding and steering, braking and thrusting motions.

The design of the torso does not impact the mobility of the legs during descending but determines the leg workspace that does not interfere with the ground surface. The contact area with the ground is maximized to reduce the robot sinking, and low-radius lateral bends allow to increase the steering capabilities. Three different



Figure 5. Image sequence of experimental trial of the Aliengo quadruped robot with custom-designed lower torso (version 1) sliding down an approximately 10m tall pile of pebbles with the help of swimming motion (from left to right, time between frames: 4s).

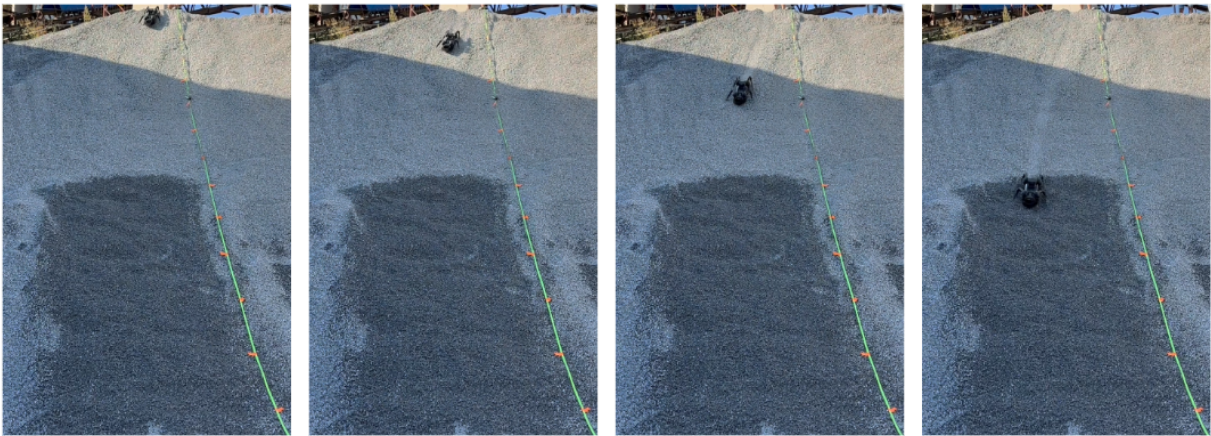


Figure 6. Image sequence of experimental trial of the Aliengo quadruped robot with custom-designed lower torso (version 2) sliding down an approximately 10m tall pile of pebbles without the need of swimming motion (from left to right, time between frames: 0.75s). The orange tape on the green rope is positioned every 1m and helps for a simple video analysis of the robot velocity.



Figure 7. Image sequence of experimental trial of the Aliengo quadruped robot with custom-designed lower torso (version 3) sliding down an approximately 10m tall pile of pebbles without the need of swimming motion (from left to right, time between frames: 1.25s).

preliminary custom-shaped lower torso were designed for the quadruped robot Aliengo: the first two differ in their round front for a low-resistance descent whilst the third one adds skids to stabilize the sliding direction.

To steer, brake and thrust during descending motions, a novel sliding locomotion control is implemented using the legs and impedance control. Each foot receives desired position and velocity references according to the sliding control commands for steering, braking and thrusting. The sliding posture is chosen taking into account not only the undesired interaction between the feet and the ground during pure sliding, but also the legs motion. A simple motion generator providing kinematic references at the Cartesian level is implemented for achieving the desired motions. The steering, braking and thrusting forces are managed through the joint impedance controller because the contact interaction between the terrain surface and the robot feet are unknown and dynamic.

We performed a multi-days field test campaign, testing sliding motions on an approximately 10m tall pile of pebbles with a grain diameter between 8 and 15mm. The robot was successfully able to slide down the steep slope. The steering motion was the most difficult to perform. The best performance was achieved with the second design with tapered and inclined front. With the third design the robot could barely twist. The braking motion is the least problematic of the three commands in terms of performance. The thrusting performance assessment follows very similar observations as for the braking motion in terms of torso design. But from the second design, there was an increase in the leg clearance from the ground. Partial surface collapse events represent also a major challenge for controlling the sliding motion.

In future works, we will explore smaller grain sizes including sand that approaches material properties of regolith. Additionally, we will optimize the torso shape, based on our experimental findings and physics simulations of the interaction between the torso and the granular media, as well as the exploration of alternative materials for the torso that reduce wear on abrasive regolith. As far as the control is concerned, we aim to improve the steering control performance by generating more complex and adequate foot trajectories and exploiting the leg joint impedances.

## ACKNOWLEDGMENTS

We would like to thank all the people at the Dynamic Legged Systems (DLS) lab of IIT that supported us for this work, and especially to Lorenzo Giustozzi for the excellent support with the organization and execution of the field trials. A special thank to Grandi Calcestruzzi Sas (Genova) as well, for giving us access to their site allowing the conduction of experiments on the inclined pile of pebbles.

## REFERENCES

- [1] Wagner, R., Robinson, M., Speyerer, E., & Mahanti, P., Topography of 20-km diameter craters on the moon. 2013, in Lunar and Planetary Science Conference
- [2] Dettmann, A., Planthaber, S., Bargsten, V., et al., Towards a Generic Navigation and Locomotion Control System for Legged Space Exploration. 2022, in ASTRA Conference
- [3] Kolvenbach, H., Arm, P., Hampp, E., et al., Traversing Steep and Granular Martian Analog Slopes With a Dynamic Quadrupedal Robot. 2022, Field Robotics
- [4] Dirk, S. & Frank, K., The Bio-Inspired SCORPION Robot: Design, Control Lessons Learned. 2007, in Climbing and Walking Robots
- [5] Bartsch, S., Manz, M., Kampmann, P., et al., Development and Control of the Multi-Legged Robot MANTIS. 2016, in Proceedings of ISR 2016: 47th International Symposium on Robotics
- [6] Bartsch, S., Development, Control, and Empirical Evaluation of the Six-Legged Robot SpaceClimber Designed for Extraterrestrial Crater Exploration. 2013, PhD thesis, University of Bremen
- [7] Roennau, A., Heppner, G., Nowicki, M., & Dillmann, R., LAURON V: A Versatile Six-Legged Walking Robot with Advanced Maneuverability. 2014, in 2014 IEEE/ASME International Conference on Advanced Intelligent Mechatronics
- [8] Seidel, D., Hermann, M., Gumpert, T., Loeffl, F. C., & Albu-Schäffer, A. O., Using Elastically Actuated Legged Robots in Rough Terrain: Experiments with DLR Quadruped bert. 2020, 2020 IEEE Aerospace Conference
- [9] The Axel rovers, <https://www-robotics.jpl.nasa.gov/how-we-do-it/systems/the-axel-rover/>
- [10] Parness, A., Abcouwer, N., Fuller, C., et al., LEMUR 3: A limbed climbing robot for extreme terrain mobility in space. 2017, in IEEE International Conference on Robotics and Automation
- [11] Wilcox, B., Litwin, T., Biesiadecki, J., et al., ATHLETE: A cargo handling and manipulation robot for the moon. 2007, Journal of Field Robotics
- [12] Reid, W., Meirion-Griffith, G., Karumanchi, S., et al., Actively Articulated Wheel-on-Limb Mobility for Traversing Europa Analogue Terrain. 2021, in Field and Service Robotics
- [13] Bramante, L., Deffacis, M., Bussi, D., et al., The Mars Terrain Simulator: a high level measurement facility in support to the ExoMars mission. 2019, in 2019 IEEE 5th International Workshop on Metrology for AeroSpace (MetroAeroSpace), 303–308
- [14] Michaud, S., von Rohr, S., Oettershagen, P., et al., Developing and using a facility enabling characterization and qualification of planetary exploration rover mobility. 2022, in ASTRA Conference
- [15] Unitree-Aliengo, <https://www.unitree.com/en/aliengo/>